

## Metal–Organic Coordination Interactions in Fe–Terephthalic Acid Networks on Cu(100)

Steven L. Tait,<sup>\*,†</sup> Yeliang Wang,<sup>†</sup> Giovanni Costantini,<sup>†,‡</sup> Nian Lin,<sup>†,#</sup>  
Alessandro Baraldi,<sup>‡,§</sup> Friedrich Esch,<sup>§</sup> Luca Petaccia,<sup>||</sup> Silvano Lizzit,<sup>||</sup> and  
Klaus Kern<sup>†,⊥</sup>

Max Planck Institute for Solid State Research, Heisenbergstrasse 1, D-70569 Stuttgart, Germany, Physics Department and Center of Excellence for Nanostructured Materials, University of Trieste, Via Valerio 2, I-34127 Trieste, Italy, Laboratorio TASC INFN-CNR, Area Science Park, I-34012 Trieste, Italy, Sincrotrone Trieste S.C.p.A., S.S. 14 Km 163.5, I-34012 Trieste, Italy, Institute de Physiques des Nanostructures, Ecole Polytechnique Fédérale de Lausanne, CH-1015 Lausanne, Switzerland, and Department of Chemistry, University of Warwick, Gibbet Hill Road, Coventry, CV47AL, United Kingdom

Received October 18, 2007; E-mail: tait@fkf.mpg.de

**Abstract:** Metal–organic coordination interactions are prime candidates for the formation of self-assembled, nanometer-scale periodic networks with room-temperature structural stability. We present X-ray photoelectron spectroscopy measurements of such networks at the Cu(100) surface which provide clear evidence for genuine metal–organic coordination. This is evident as binding energy shifts in the O 1s and Fe 3p photoelectron peaks, corresponding to O and Fe atoms involved in the coordination. Our results provide the first clear evidence for charge-transfer coordination in metal–organic networks at surfaces and demonstrate a well-defined oxidation state for the coordinated Fe ions.

### Introduction

Supramolecular self-organization is a strategy of growing interest for efficient and uniform patterning of surfaces with periodic nanometer-scale structures.<sup>1</sup> Effective assembly of molecular networks requires intercomponent interactions that are sufficiently robust to stabilize the desired structure but also sufficiently labile to allow error correction during growth. It has been demonstrated in recent scanning tunneling microscopy (STM) studies that metal–organic coordination systems are a prime candidate for the formation of such two-dimensional (2D) structures at surfaces,<sup>2,3</sup> analogous to their use in three-dimensional (3D) supramolecular organization in solution based chemistry.<sup>4</sup> Supramolecular coordination interactions within the metal–organic structures are strong enough to allow stability

at room temperature and above, yet reversible enough to allow ligands to detach from structural defects, i.e., to allow structural error correction by molecular level self-selection.<sup>5</sup>

Coordination of terephthalic acid (TPA) with Fe centers at the Cu(100) surface is a model system for study of coordination networks at surfaces. This system has been investigated extensively by STM, providing excellent structural characterization of the several TPA + Fe phases which are observed at different Fe/TPA ratios.<sup>6</sup> However, the STM is not able to directly characterize the charge state or local chemical environment of the network components. It has been assumed, based on STM structural measurements and analogous structures in solution based chemistry, that the stabilizing interaction for these networks is a coordination bonding involving charge transfer between the Fe centers and the functional groups of the organic ligands, but direct evidence has not yet been provided. Here we present measurements of the electron core level binding energies (BE) of the Fe centers and of the O atoms in the carboxylate functional groups. Resolution of characteristic core level shifts due to changes in the local chemical environment is one of the strong features of the X-ray photoelectron spectroscopy (XPS) technique.<sup>7,8</sup> Our measurements provide evidence for the coordination nature of the interaction between

<sup>†</sup> Max Planck Institute for Solid State Research.

<sup>‡</sup> University of Trieste.

<sup>§</sup> Laboratorio TASC INFN-CNR.

<sup>||</sup> Sincrotrone Trieste S.C.p.A.

<sup>⊥</sup> Ecole Polytechnique Fédérale de Lausanne.

<sup>○</sup> University of Warwick.

<sup>#</sup> Present address: Department of Physics, The Hong Kong University of Science and Technology, Clear Water Bay, Kowloon, Hong Kong, China.

(1) Barth, J. V.; Costantini, G.; Kern, K. *Nature* **2005**, *437*, 671.

(2) Dmitriev, A.; Spillmann, H.; Lin, N.; Barth, J. V.; Kern, K. *Angew. Chem., Int. Ed.* **2003**, *42*, 2670.

(3) Stepanow, S.; Lin, N.; Barth, J. V.; Kern, K. *J. Phys. Chem. B* **2006**, *110*, 23472; Spillmann, H.; Dmitriev, A.; Lin, N.; Messina, P.; Barth, J. V.; Kern, K. *J. Am. Chem. Soc.* **2003**, *125*, 10725.

(4) Lehn, J. M. *Supramolecular Chemistry. Concepts and Perspectives*; VHC: Weinheim, Germany, 1995. Holliday, B. J.; Mirkin, C. A. *Angew. Chem., Int. Ed.* **2001**, *40*, 2022. Swiegers, G. F.; Malefetse, T. *J. Chem. Rev.* **2000**, *100*, 3483. Leininger, S.; Olenyuk, B.; Stang, P. J. *Chem. Rev.* **2000**, *100*, 853. Lawrence, D. S.; Jiang, T.; Levett, M. *Chem. Rev.* **1995**, *95*, 2229.

(5) Tait, S. L.; Langner, A.; Lin, N.; Stepanow, S.; Rajadurai, C.; Ruben, M.; Kern, K. *J. Phys. Chem. C* **2007**, *111*, 10982. Langner, A.; Tait, S. L.; Lin, N.; Rajadurai, C.; Ruben, M.; Kern, K. *Proc. Natl. Acad. Sci. U.S.A.* **2007**, *104*, 17927.

(6) Lingenfelder, M. A.; Spillmann, H.; Dmitriev, A.; Stepanow, S.; Lin, N.; Barth, J. V.; Kern, K. *Chem.—Eur. J.* **2004**, *10*, 1913.

(7) Baraldi, A.; Comelli, G.; Lizzit, S.; Kiskinova, M.; Paolucci, G. *Surf. Sci. Rep.* **2003**, *49*, 169.

the Fe centers and the ligands, confirming the presumed bonding motif suggested in prior STM<sup>2,6,9</sup> and X-ray absorption spectroscopy (XAS)<sup>10</sup> studies. A well-defined chemical shift is identified for the coordinated Fe atoms, and the value of that shift is consistent with prior measurements of iron oxides in a +2 oxidation state.

## Experimental Section

The photoemission studies were performed at the SuperESCA beamline<sup>7,11</sup> of the ELETTRA third generation synchrotron radiation source in Trieste, Italy. The experimental chamber is equipped with a double pass hemispherical electron energy analyzer with a 96 channel detector<sup>12</sup> and has a background pressure of about  $2 \times 10^{-10}$  mbar. The Cu(100) single crystal was cleaned by cycles of Ar<sup>+</sup> ion sputtering at room temperature ( $E = 500$  eV) and flash annealing to 800 K. Surface cleanliness was verified by inspecting C 1s, Cu 3p, Fe 3p, and O 1s XPS signals as well as the low-energy electron diffraction (LEED) pattern. Core level spectra were recorded with the sample at room temperature and at a photon energy of 203 eV (Fe 3p, Cu 3p), 396 eV (C 1s), or 650 eV (O 1s), with an overall energy resolution of better than 100–250 meV.<sup>7</sup> Core level spectra binding energies were referenced to the Fermi level.

Other XPS studies of iron species have concentrated on Fe 2p<sub>3/2</sub> spectra, where energy contrast is higher for chemical shifts (2.6–3.1 eV for Fe<sup>2+</sup> and 4.0–4.2 eV for Fe<sup>3+</sup>)<sup>13–16</sup> compared to the same shifts in the Fe 3p peaks (1.5–1.9 eV and 2.7–2.9 eV, respectively).<sup>15–18</sup> However, we chose to study the Fe 3p peaks to take advantage of higher photon flux and better energy resolution available at the lower photon energy on the ELETTRA SuperESCA beamline.

The organic ligand terephthalic acid (TPA, benzene-1,4-dicarboxylic acid, C<sub>6</sub>H<sub>4</sub>(COOH)<sub>2</sub>), purchased from Fluka Chemie GmbH, was deposited from a Knudsen cell held at 450 K giving a molecule flux of approximately 0.6 ML/min at the sample. Fe was evaporated from an electron-beam evaporator with a deposition rate of ~0.03 ML/min. The amount of each deposited component was controlled accurately by the evaporation source temperature and the shutter-open time and was always in submonolayer quantities, except for the multilayer Fe films noted below. All depositions were made with the substrate at room temperature. In the case of TPA–Fe mixtures, TPA was deposited before Fe and the sample was subsequently annealed to 410 K for several minutes.

The XPS analysis was done by fitting the core level spectra with a Doniach–Šunjić (DS) function,<sup>19</sup> characterized by two parameters: the singularity index  $\alpha$  (describing the peak asymmetry due to the final-state screening of the core-hole) and the Lorentzian width  $\Gamma$  (because of the finite core-hole lifetime), convoluted with a Gaussian of width

$G$  (to account for instrumental resolution and phonon broadening/vibrational fine structure). A linear background was also subtracted.

## Results and Discussion

When TPA molecules are evaporated on the clean Cu(100) surface at room temperature, they show sufficient mobility and intermolecular attraction to order themselves into a very regular and rather dense structure (Figure 1c). This structure gives a sharp ( $3 \times 3$ ) LEED pattern indicating a square, commensurate TPA overlayer structure which has a real-space lattice spacing three times larger than the Cu(100) lattice structure and is aligned with the [011] direction of the surface (Figure 1a). Clearly visible in this figure are the (1,0) spots from the underlying Cu substrate (circled in Figure 1a). A schematic model of this structure, consistent with prior STM results (Figure 1c),<sup>6</sup> is shown in Figure 1b. The TPA molecules are drawn with the aromatic ring centered over the fourfold hollow sites of the substrate, as predicted in previous calculations.<sup>20</sup> The orientation of the molecule axis parallel to the [101] direction of the substrate provides the possibility for ionic O<sup>••</sup>H–C hydrogen bond interactions<sup>21</sup> between neighboring TPA molecules.

This ionic hydrogen bonding is facilitated by deprotonation of the TPA carboxylate groups. Core level spectra indicate that upon deposition at room temperature, the majority (>80%) of the TPA carboxylate groups are deprotonated. After annealing to 410 K, the molecules are completely deprotonated and the ( $3 \times 3$ ) LEED pattern becomes sharper and brighter. The protonated groups are evident in an O 1s core level peak 2 eV higher BE than the deprotonated O peak (531.0 eV). There is a corresponding, although less noticeable, transition in the C 1s core level peaks. These core level shifts due to deprotonation are consistent with a previous study of TPA at low (190 K) and high (400 K) temperatures on Cu(100).<sup>22</sup>

Subsequent deposition of Fe atoms onto a surface containing deprotonated TPA molecules, along with thermal annealing at 410 K, allows the TPA and Fe to form well-ordered 2D network structures on the surface.<sup>6</sup> At small Fe coverages, we find a well-defined LEED pattern indicating a ( $6 \times 6$ ) overlayer structure, as shown in Figure 1d. STM investigations<sup>6</sup> have revealed that at low Fe/TPA ratios (~1:4) a periodic arrangement of Fe(TPA)<sub>4</sub> “cloverleaf” coordination units with a periodicity six times greater than that of the Cu(100) substrate is formed (see Figure 1e and f). The Fe ion coordination centers are expected to prefer the fourfold hollow adsorption sites on Cu(100). Four TPA molecules are arranged around a single Fe center so that for each TPA molecule there is one oxygen coordinated to the Fe center while the other three are ionically hydrogen bonded (O<sup>••</sup>H–C) to neighboring molecules (see model, Figure 1e).<sup>6</sup>

At higher Fe/TPA ratios, the LEED pattern becomes diffuse (Figure 1g). Corresponding STM studies showed that the additional Fe allows for the formation of structures where a higher number of O–Fe coordination bonds are formed, leading to several local supramolecular arrangement possibilities (e.g.,

- (8) Flechtner, K.; Kretschmann, A.; Bradshaw, L. R.; Walz, M. M.; Steinruck, H. P.; Gottfried, J. M. *J. Phys. Chem. C* **2007**, *111*, 5821. Gottfried, J. M.; Flechtner, K.; Kretschmann, A.; Lukaszczuk, T.; Steinruck, H. P. *J. Am. Chem. Soc.* **2006**, *128*, 5644.
- (9) Lin, N.; Dmitriev, A.; Weckesser, J.; Barth, J. V.; Kern, K. *Angew. Chem., Int. Ed.* **2002**, *41*, 4779. Messina, P.; Dmitriev, A.; Lin, N.; Spillmann, H.; Abel, M.; Barth, J. V.; Kern, K. *J. Am. Chem. Soc.* **2002**, *124*, 14000.
- (10) Gambardella, P.; Stepanow, S.; Dmitriev, A.; Gupta, S. S.; Honolka, J.; Clair, S.; Pons, S.; Lingenfelder, M.; Bencok, P.; Stanescu, S.; Sarma, D. D.; Lin, N.; Brune, H.; Barth, J. V.; Kern, K. In preparation.
- (11) Baraldi, A.; Barnaba, M.; Brena, B.; Cocco, D.; Comelli, G.; Lizzit, S.; Paolucci, G.; Rosei, R. *J. Electron Spectrosc. Relat. Phenom.* **1995**, *76*, 145.
- (12) Baraldi, A.; Dhanak, V. R. *J. Electron Spectrosc. Relat. Phenom.* **1994**, *67*, 211.
- (13) Brundle, C. R.; Chuang, T. J.; Wandelt, K. *Surf. Sci.* **1977**, *68*, 459.
- (14) Lesiak, B.; Jablonski, A.; Zemek, J.; Jiricek, P.; Cernansky, M. *Appl. Surf. Sci.* **2005**, *252*, 330.
- (15) McIntyre, N. S.; Zetarak, D. G. *Anal. Chem.* **1977**, *49*, 1521.
- (16) Mills, P.; Sullivan, J. L. *J. Phys. D: Appl. Phys.* **1983**, *16*, 723; Konno, H.; Nagayama, M. *J. Electron Spectrosc. Relat. Phenom.* **1980**, *18*, 341.
- (17) Paparazzo, E. *J. Electron Spectrosc. Relat. Phenom.* **2006**, *154*, 38.
- (18) Yamashita, T.; Hayes, P. *J. Electron Spectrosc. Relat. Phenom.* **2006**, *152*, 6.
- (19) Doniach, S.; Sunjic, M. *J. Phys. C: Solid State Phys.* **1970**, *3*, 285.

- (20) Chen, W. K.; Cao, M. J.; Liu, S. H.; Xu, Y.; Li, J. Q. *Chem. Phys. Lett.* **2005**, *407*, 414. Lorente, N.; Hedouin, M. F. G.; Palmer, R. E.; Persson, M. *Phys. Rev. B* **2003**, *68*.
- (21) Payer, D.; Comisso, A.; Dmitriev, A.; Strunskus, T.; Lin, N.; Woll, C.; De Vita, A.; Barth, J. V.; Kern, K. *Chem.–Eur. J.* **2007**, *13*, 3900.
- (22) Stepanow, S.; Strunskus, T.; Lingenfelder, M.; Dmitriev, A.; Spillmann, H.; Lin, N.; Barth, J. V.; Woll, C.; Kern, K. *J. Phys. Chem. B* **2004**, *108*, 19392.

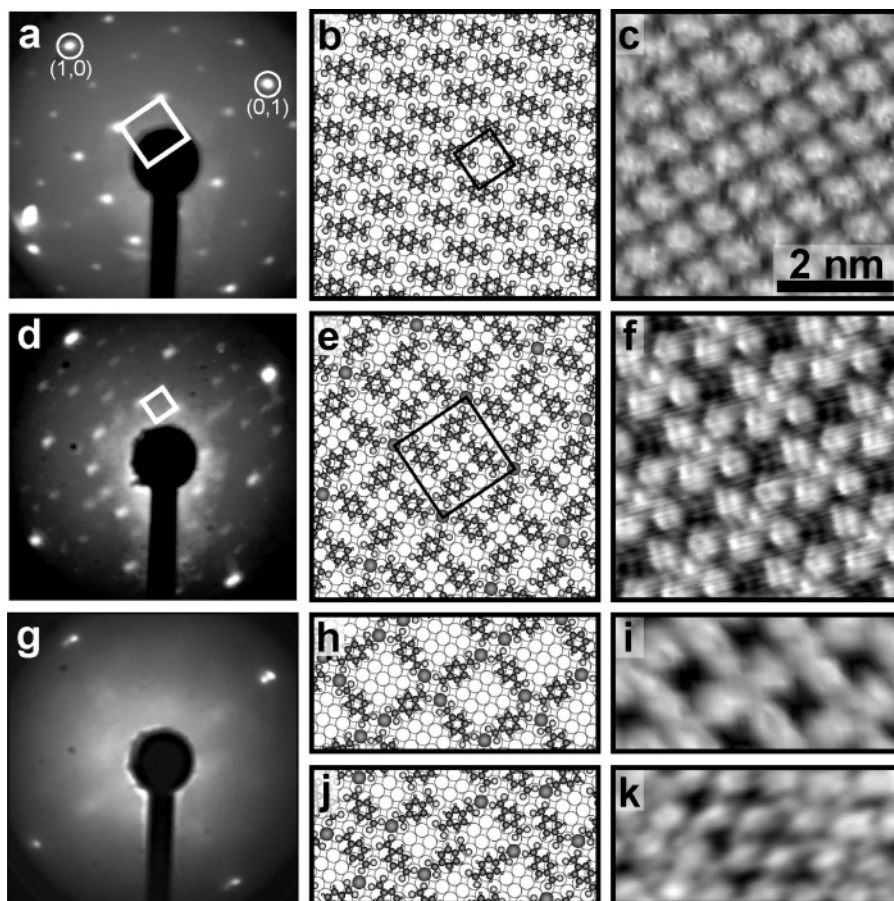


**Figure 1.** TPA and TPA–Fe structures on Cu(100). (a, d, g) LEED patterns, (b, e, h, j) structural models, and (c, f, i, k) STM images of scan width 5 nm. (a, b, c)  $3 \times 3$  pure TPA phase. Unit cell of TPA layer is indicated in (a, b), and (1,0) and (0,1) spots from the Cu(100) substrate are circled in (a). (d, e, f)  $6 \times 6$   $\text{Fe}(\text{TPA})_4$  coordination phase. (g) Diffuse LEED pattern at higher Fe coverages; only (1,0) substrate spots are visible. This is most likely due to a multiplicity of Fe–TPA coordination structures, two of which are illustrated in (h–k). LEED images recorded at (a) 82 eV and at (d, g) 69 eV. (a) has been stretched by the factor  $\sqrt{82/69}$  for direct comparison with (d) and (g). Models and STM images are similar to those reported previously.<sup>6</sup>

Figure 1h–k).<sup>6</sup> The local structural information provided by STM shows that a variety of such structures coexist on the surface, which explains why LEED measurements, which are effectively a structural average over a wider surface region, do not produce sharp spots for the overlayer.

The structural stability of the highly ordered TPA–Fe coordination networks has been attributed to coordination bonding involving Fe ions.<sup>2,6,9</sup> Such a charge transfer interaction is expected to be evident in core level spectra. Figure 2a displays five O 1s spectra from a single experiment, i.e., a single TPA deposition step with subsequent incremental Fe depositions. The bottom-most spectrum was made before any Fe deposition and therefore corresponds to the  $(3 \times 3)$  TPA structure, in which nearly all O atoms are involved in hydrogen bonding with neighboring molecules (see Figure 1b and c). The single O 1s feature at 531.0 eV corresponds to the fully deprotonated carboxylate moieties. In the subsequent XPS measurements with increasing Fe (moving up in the figure), this feature is observed to broaden. In the analysis of these data, we fit the spectra to two peaks: the first is fixed at 531.0 eV (determined from pure TPA experiments). The second peak position is free in the fitting procedure, but its shape (width and asymmetry parameters:  $\Gamma$ ,  $G$ , and  $\alpha$ ) is forced to be the same as that for the first peak. In each of these cases, the best fits were obtained with the second peak position at  $531.6 \pm 0.1$  eV (error represents one standard

deviation), i.e., with the second peak having virtually the same position for all of the spectra. Therefore, the O 1s spectra demonstrate the existence of two distinct, well-defined chemical states for the carboxylate O atoms of TPA: uncoordinated (531.0 eV) and Fe-coordinated (531.6 eV).

At first glance, it seems unusual that the O 1s peaks (electron acceptor) would shift to higher binding energy upon coordination to Fe. This apparent inconsistency can be understood by considering that in the initial, “uncoordinated” state the carboxylate groups are nearly all involved in hydrogen bonding to surrounding molecules (see Figure 1b) and are also expected to have some interaction with the Cu atoms in the underlying substrate. Upon coordination to Fe the carboxylate moiety must give up the hydrogen bonding and their interactions with the substrate atoms may be significantly affected as well. Apparently, electron donation from the Fe centers and substrate atoms to the “coordinated” TPA is less efficient compared to electron donation from the hydrogen bonding and substrate atoms to the “uncoordinated” TPA. Therefore, the O 1s core levels have a higher binding energy in the coordinated state compared to the “uncoordinated” state. Additionally, we cannot exclude that final state effects can contribute to the observed O 1s binding energy changes: indeed a weakening of the O–Cu(100) bond may reduce the efficiency of the screening of the core-hole, resulting in a shift to higher binding energy.



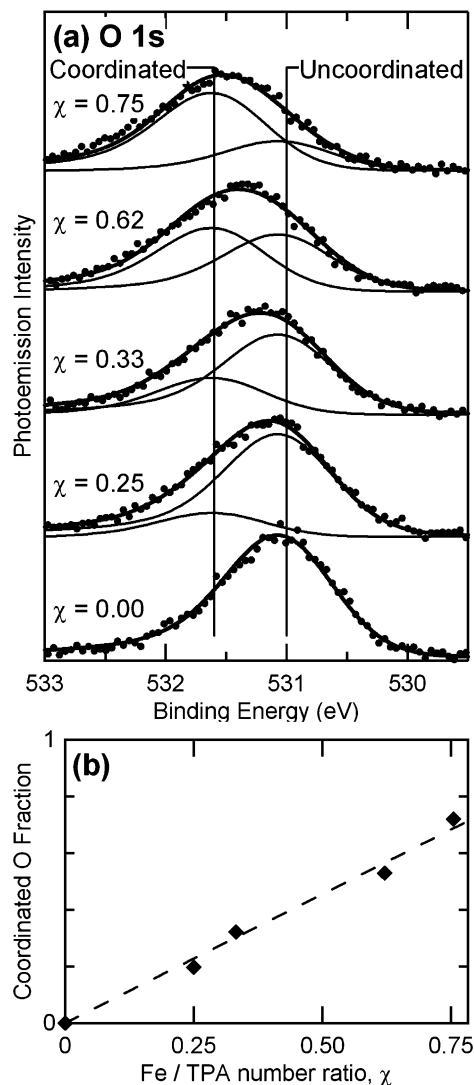


**Figure 2.** O 1s XPS spectra of TPA on Cu(100) with codeposited Fe. The value  $\chi$  represents the Fe/TPA number ratio, as described in the text. (a) Spectra at various  $\chi$  values showing the growth of a high binding energy (531.6 eV) feature at the expense of the single feature observed for pure TPA (531.0 eV). The total O 1s area is constant. The high binding energy component is attributed to O which is coordinated to Fe ions. (b) Plot of the fraction of coordinated carboxyl group O atoms vs the Fe/TPA number ratio.

As the amount of Fe increases, the amplitude of the O 1s peak at 531.0 eV (uncoordinated O) decreases, while the peak at 531.6 eV (coordinated O) correspondingly increases (the total area of the O 1s peaks remains constant at constant TPA coverage). This is quantitatively represented in Figure 2b where the fraction of TPA oxygen sites involved in Fe coordination is plotted versus the Fe/TPA ratio on the surface. The values on the vertical axis, representing the coordinated O fraction, are calculated as the ratio between the area of the 531.6 eV BE peak and the total O 1s area. The Fe/TPA number ratio  $\chi$ , displayed on the horizontal axis, is calculated by dividing the Fe 3p peak area by the O 1s peak area and normalizing the resulting ratio so that  $\chi = 0.25$  for the experiment with the ( $6 \times 6$ ) LEED pattern [Fe(TPA)<sub>4</sub> “cloverleaf” phase, Figure 1d]. This normalization assumes that the ( $6 \times 6$ ) LEED was produced from exactly a 1:4 Fe/TPA number ratio and therefore represents only an approximate number ratio.

In Figure 2b, the fraction of O atoms that switches from the uncoordinated to the coordinated state proceeds in an approximately linear manner with the Fe/TPA ratio up to a value of  $\chi$  of about 0.7–0.8. This result indicates that most of the deposited Fe is occupied in coordination interactions to the TPA molecules up to that coverage. This agrees well with the observations of Clair and co-workers:<sup>23</sup> the molecules are mobile on the surface to find a metal coordination center, even taking atoms from metal clusters, if necessary. For very large amounts of Fe, it becomes difficult for the TPA and Fe to mix perfectly, due to steric limitations that reduce two-dimensional mobility and because of the few available carboxyl coordination sites, and so some of the Fe is left uncoordinated. At higher Fe/TPA ratios (>0.8), we indeed observed that the increase in the coordinated fraction of O shows a more asymptotic behavior as it approaches unity.

Evidence for Fe–TPA coordination is also clear from the behavior of the Fe 3p XPS peaks. In Figure 3a we have plotted the Fe 3p photoemission spectra for samples containing TPA and increasing amounts of Fe [spectra (i–v)] as well as for a film of Fe grown on a clean Cu(100) surface [spectrum (vi)]. Spectra (i–iv) were recorded in the same experiment as the upper four curves in Figure 2a with corresponding  $\chi$  values. Spectrum (i) has the correct Fe/TPA ratio to produce the ( $6 \times 6$ ) cloverleaf structure, and curves above are for additional Fe exposures, increasing Fe coverage moving up in Figure 3a. The intensity of these spectra is relatively low due to the low absolute coverage of Fe on the surface.<sup>24</sup> Spectrum (v) was a separate experiment in which the sample was prepared with 50% less TPA and a large Fe exposure, so that there is a significant excess of Fe on the sample. Spectrum (vi) was again a separate experiment; in this case there was no TPA deposition, and a multilayer Fe film was evaporated to the surface.

The Fe 3p feature for the Fe multilayer film in Figure 3a(vi) is fitted well by two components at 52.8 and 52.0 eV. The shape and position of this peak and the two peak fit are consistent with previous XPS studies on metallic Fe<sup>0</sup> thin films.<sup>25</sup> This relatively simple two peak fit neglects the underlying complexity of the Fe 3p peak structure due to electron exchange interaction and electron correlation effects which have been explored in detail previously.<sup>17,26,27</sup>

The coordination of the Fe atoms to the TPA molecules leads to a different Fe 3p photoemission feature which is shifted to higher binding energy with respect to the Fe metal peak. In order to fit this new feature, we assume that the Fe 3p photoelectron emission spectrum should have the same structure for coordinated Fe as for the metallic Fe. This is a reasonable

- (23) Clair, S.; Pons, S.; Fabris, S.; Baroni, S.; Brune, H.; Kern, K.; Barth, J. V. *J. Phys. Chem. B* **2006**, *110*, 5627. Clair, S.; Pons, W.; Brune, H.; Kern, K.; Barth, J. V. *Angew. Chem., Int. Ed.* **2005**, *44*, 7294.
- (24) The  $6 \times 6$  structure corresponding to spectrum 3(i) contains only one Fe atom per 36 substrate Cu atoms, i.e. an Fe number density of  $4.27 \times 10^{13} \text{ cm}^{-2}$ .
- (25) Handke, B.; Simonsen, J. B.; Bech, M.; Li, Z. S.; Moller, P. J. *Surf. Sci.* **2006**, *600*, 1123. Van Campen, D. G.; Pouliot, R. J.; Klebanoff, L. E. *Phys. Rev. B* **1993**, *48*, 17533. Roth, C.; Hillebrecht, F. U.; Rose, H. B.; Kisker, E. *Phys. Rev. Lett.* **1993**, *70*, 3479. Sinkovic, B.; Johnson, P. D.; Brookes, N. B.; Clarke, A.; Smith, N. V. *J. Appl. Phys.* **1991**, *70*, 5918.
- (26) Gupta, R. P.; Sen, S. K. *Phys. Rev. B* **1974**, *10*, 71. Bagus, P. S.; Freeman, A. J.; Sasaki, F. *Phys. Rev. Lett.* **1973**, *30*, 850. Fadley, C. S.; Shirley, D. A. *Phys. Rev. A* **1970**, *2*, 1109. Fadley, C. S.; Shirley, D. A.; Freeman, A. J.; Bagus, P. S.; Mallow, J. V. *Phys. Rev. Lett.* **1969**, *23*, 1397. Rossi, G.; Sirotti, F.; Cherepkov, N. A.; Farnoux, F. C.; Panaccione, G. *Solid State Commun.* **1994**, *90*, 557.
- (27) Grosvenor, A. P.; Kobe, B. A.; Biesinger, M. C.; McIntyre, N. S. *Surf. Inter. Anal.* **2004**, *36*, 1564.

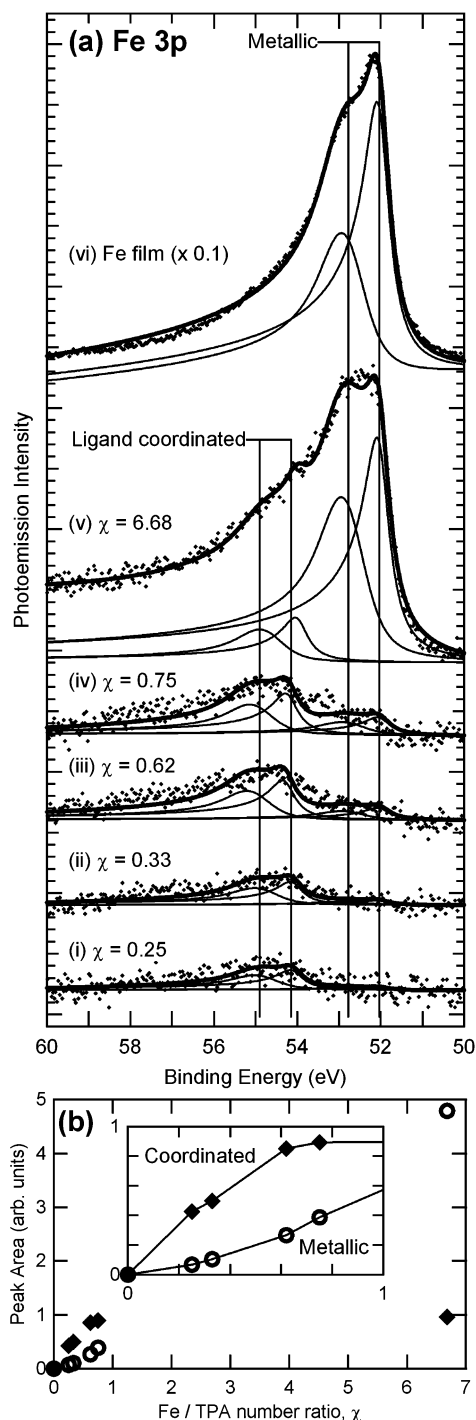


**Figure 3.** (a) Fe 3p XPS spectra: (i–iv) same experiment as the top four O 1s spectra in Figure 2a; (v) separate experiment with 50% less TPA and five times more Fe than (iv), i.e., a significant excess of Fe beyond that needed for TPA coordination; (vi) multilayer Fe (metallic) film on Cu(100) with no TPA, reduced  $10\times$  for clarity of presentation. Spectra (i–v) are each fit with the same pair of peaks as for metallic Fe in (vi) as well as a duplicate pair of peaks shifted by 2.1 eV, which correspond to TPA-coordinated Fe atoms. Vertical lines drawn at peak positions differ from peak maxima due to asymmetry factor. (b) Peak pair areas for metallic (O) and coordinated (◆) Fe in (a) vs the Fe/TPA number ratio,  $\chi$ . Inset: detail at small  $\chi$ .

choice, supported by the fact that the detailed photoemission structure has been shown to be unchanged for iron oxides and other iron compounds compared to metallic iron.<sup>13,15,27</sup> The assumption of this complex peak shape compared to a simpler

fitting curve does not affect the conclusions of this study (see Supporting Information). Spectra (i–v) were each fit with two sets of the peak pair fitted to (vi). The spectra are fitted well with the first peak pair at the position for the metallic Fe in spectrum (vi). The position of the second peak pair for the fits to spectra (i–v) was 54.1 and 54.9 eV ( $\pm 0.1$  eV). This peak pair, shifted from metallic Fe by 2.1 eV, corresponds to the Fe which is involved in coordination interactions to the organic molecules.

Spectrum (v) in Figure 3a represents a superposition of the Fe metal film peak with the coordinated Fe peak. This demonstrates, on a single sample, the relative BE positions of the metallic Fe<sup>0</sup> 3p peak and the peak of the Fe centers involved in coordination to the functional carboxylate groups of the TPA molecules ( $\Delta BE = 2.1$  eV). Evaluation of the energy shift in the Fe core level peaks upon coordination is in some sense more straightforward than the interpretation of the O 1s discussed above, because here we are comparing a shift relative to a metallic Fe film (charge neutral state). This energy shift is in very good agreement with a previous study of Fe metal, FeO, and Fe<sub>2</sub>O<sub>3</sub> which found shifts in Fe 3p of 1.9 for Fe<sup>2+</sup> (and 2.7 eV for Fe<sup>3+</sup>).<sup>15</sup> Thus, the significant shift in the Fe XPS peak is consistent with earlier predictions that the coordinated Fe centers are ionized<sup>2,6,9,10,28</sup> and further demonstrates that there is a well-defined oxidation state for the coordinated Fe atoms on the surface; that is, the oxidation state does not shift significantly with changing  $\chi$ . Prior DFT calculations found that in these Fe–TPA coordination systems on Cu(100) the Fe centers are lifted by 0.6 Å from the fourfold hollow sites.<sup>28</sup> However, even though the interaction of Fe with the Cu substrate is diminished upon coordination, there remains a substantial electronic hybridization between the Fe centers and substrate as calculated by DFT<sup>28</sup> and observed for similar metal centers in porphyrin compounds at metal surfaces.<sup>29</sup> The magnitude of the observed chemical shift of the Fe core level energy is consistent with that observed for iron oxides in a +2 oxidation state.<sup>15</sup> However, this similarity in the core-level shift does not necessarily imply an identical chemical environment, due to the presence of the metallic substrate.

In Figure 3b, we have plotted the normalized areas for each of the peak pairs, metallic Fe and coordinated Fe corresponding to spectra (i–v) in Figure 3a. The peak area of the ligand coordinated Fe increases rapidly at first, but then it reaches a saturation level around  $\chi = 0.7$ – $0.8$ . The metallic Fe photoemission intensity increases slowly at first then more rapidly, indicating that, even before the Fe coordination intensity reaches saturation, there is some metallic Fe which is left uncoordinated at the surface. Some portion of this metallic Fe signal may be due to inefficient mixing of the coordination components at the surface, but certainly a significant fraction can be attributed to the known effect of interdiffusion of the Fe adatoms with the Cu substrate at these temperatures.<sup>6,30</sup>

- (28) Seitsonen, A. P.; Lingenfelder, M.; Spillmann, H.; Dmitriev, A.; Stepanow, S.; Lin, N.; Kern, K.; Barth, J. V. *J. Am. Chem. Soc.* **2006**, *128*, 5634.  
 (29) Flechtner, K.; Kretschmann, A.; Steinruck, H. P.; Gottfried, J. M. *J. Am. Chem. Soc.* **2007**, *129*, 12110. Lukaszczuk, T.; Flechtner, K.; Merte, L. R.; Jux, N.; Maier, F.; Gottfried, J. M.; Steinruck, H. P. *J. Phys. Chem. C* **2007**, *111*, 3090. Leung, K.; Rempe, S. B.; Schultz, P. A.; Sproviero, E. M.; Batista, V. S.; Chandross, M. E.; Medforth, C. J. *J. Am. Chem. Soc.* **2006**, *128*, 3659. Scudiero, L.; Barlow, D. E.; Mazur, U.; Hipps, K. W. *J. Am. Chem. Soc.* **2001**, *123*, 4073. Scudiero, L.; Barlow, D. E.; Hipps, K. W. *J. Phys. Chem. B* **2000**, *104*, 11899.  
 (30) Spisak, D.; Hafner, J. *Phys. Rev. B* **2001**, *64*, 205422. Chambliss, D. D.; Johnson, K. E. *Phys. Rev. B* **1994**, *50*, 5012.

## Conclusions

We have applied X-ray photoelectron spectroscopy measurements to studies of self-assembled metal–organic networks at surfaces. Our results provide chemical resolution of the interactions which stabilize the highly ordered nanometer-scale networks observed by STM. LEED measurements confirm the  $(3 \times 3)$  structure of pure TPA layers and the  $(6 \times 6)$  structure of TPA–Fe coordination systems at low (1:4) Fe/TPA ratios on Cu(100). XPS measurements clearly demonstrate that the mixing of TPA and Fe has a strong impact on the Fe electronic core levels, indicating a significant electronic interaction between the Fe centers and the TPA molecules. Electron core level binding energy shifts in the O 1s peaks with increasing Fe exposure show that these interactions occur through Fe–O coordination at the deprotonated carboxylate groups, as expected from STM topographical measurements. Clearly resolved in the O 1s spectra is a shift of 0.6 eV to higher binding energy due to coordination of the O atoms in the carboxylate groups to the Fe centers. Fe 3p spectra show a shift of 2.1 eV to higher

binding energy for Fe atoms which are involved in coordination to the TPA ligands and indicate a well-defined oxidation state for these coordination centers. These results demonstrate Fe–TPA coordination bonding at the Cu(100) surface. Although there are several complexities due to the presence of the metal substrate, this charge-transfer coordination bonding at surfaces shows some analogous behavior to the interactions stabilizing solution based (3D) metal–organic coordination systems: charge-transfer coordination interactions and selective and directional bonding, which leads to highly ordered coordination architectures.

**Acknowledgment.** We would like to thank G. Comelli for stimulating discussions. S.L.T. gratefully acknowledges support from the Alexander von Humboldt Foundation.

**Supporting Information Available:** Detailed information regarding the peak fitting for the Fe 3p data. This material is available free of charge via the Internet at <http://pubs.acs.org>.

JA0778186